Magnetoelastic clock system for NanoMagnet Logic

Marco Vacca, Mariagrazia Graziano, *Member IEEE,* L. Di Crescenzo, A. Chiolerio, A. Lamberti, D. Balma, G. Canavese, F. Celegato, E. Enrico, P. Tiberto, L. Boarino, M. Zamboni

Abstract—In recent years magnetic-based technologies, like NanoMagnet Logic (NML), are gaining increasing interest as possible substitutes of CMOS transistors. The possibility to mix logic and memory in the same device, coupled with a potential low power consumption, opens up completely new ways of developing circuits. The major issue of this technology is the necessity to use an external magnetic field as clock signal to drive the information through the circuit. The power losses due to the magnetic field generation potentially wipe out any advantages of NML logic. To solve the problem new clock mechanisms were developed, based on spin-transfer torque current and on voltage-controlled multiferroic structures that use magnetoelastic properties of magnetic materials, i.e. exploiting the possibility of influencing magnetization dynamics by means of the elastic tensor. In particular the latter shows an extremely low power consumption.

In this paper we propose an innovative voltage-controlled magnetoelastic clock system aware of the technological constraints risen by modern fabrication processes. We show how circuits can be fabricated taking into account technological limitations and we evaluate the performance of the proposed system. Results show that the proposed solution promises remarkable improvements over other NML approaches, even though state-of-the-art ideal multiferroic logic has in theory better performance. Moreover, since the proposed approach is technology-friendly, it gives a substantial contribution toward the fabrication of a full magnetic circuit and represents an optimal trade off between performance and feasibility.

Index Terms—NanoMagnets Logic, Magneto-Elastic effect, Low Power

I. INTRODUCTION

The continuous scaling of transistors is the reason behind the incredible development that CMOS technology has undergone in the last decades. While this scaling process is reaching its physical limits, new technologies are studied as possible CMOS substitutes. Particularly, magnetic-based technologies are of increasing interest due to the very low power consumption expected and the possibility to combine memory and logic in the same device. Among these technologies, NanoMagnet Logic (NML) was one of the first studied and demonstrated at experimental level [1][2][3]. Single domain nanomagnets, which have only two stable states thanks to magnetic anisotropy, are used to represent the logic values

M. Vacca, M. Graziano L. Di Crescenzo and M. Zamboni are with the Electronics and Telecommunications Department of Politecnico di Torino, Italy. A. Chiolerio and A. Lamberti are with Istituto Italiano di Tecnologia (IIT), Center for Space Human Robotics, Torino, Italy and Chilab - Materials and Microsystems Laboratory, Chivasso, Italy. D. Balma is with the cole Polytechnique Federale de Lausanne, Ceramics Laboratory, Lausanne, Switzerland. F. Celegato, E. Enrico, P. Tiberto and L. Boarino are with Istituto Nazionale per la Ricerca Metrologica (INRIM), Torino, Italy

"0" and "1" (Figure 1.A). Circuits are built placing magnets in close proximity to each other: To reach the minimum energy state horizontally coupled magnets align themselves antiferromagnetically, while vertically coupled magnets align themselves ferromagnetically [4], as can be seen from Figure 1.A. We also demonstrated that even a multidomain element may behave in a similar way, in the so called Quasi-Single Domain Logic (QSDL), helping to reach interesting results with low resolution cost-effective lithographic capabilities [5]. In this way information propagates through the circuit and logic gates can be built. In particular, by changing the shape of the magnets it is possible to build AND/OR gates [6]. Moreover, exploiting the antiferromagnetic coupling of horizontally placed magnets, it is possible to implement an inverter by placing an odd number of magnets in a row [4]. NML circuits shows also a good tolerance to process variations [7] due to errors in the fabrication processes [8][9].
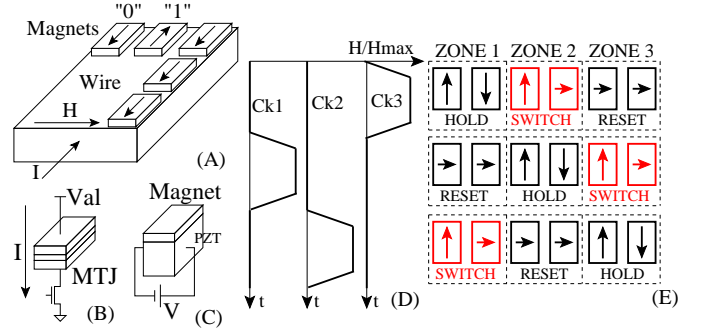

Fig. 1. NanoMagnet Logic fundamentals. A) Single domain nanomagnets are used to represent the logic values "0" and "1". In the classical approach a current which flows through a wire placed under the magnets plane generates the magnetic field that is used has clock signal. B) STT-current induced clocking for NML logic. MTJs junctions are used as basic elements and a current flowing through the magnets is used as clock. C) Multiferroic NML logic. The basic elements is a multilayered structure made by a piezoelectric material and a magnetic layer. D) Multiphase clock system. Three clock signals with a phase difference of 120 degrees are applied to specific area of the circuit called clock zones. E) Magnetization evolution in a NML circuit where the multiphase clock system is applied.

Unfortunately, an external magnetic field is necessary to help the magnets to switch from one stable state to the other [10]. This magnetic field in the most classical approach is generated by a current (I) flowing through a wire placed under the magnets plane (Figure 1.A). The generated magnetic field is therefore parallel to the short side of the magnets, so when it is applied, magnets are forced in an intermediate unstable state with the magnetization vector rotated along the short side. When the magnetic field is removed magnets realign themselves following the input magnet. This mechanism is called "clock" [4]. Several solutions have been proposed in

literature, as discussed in section II, based on current induced magnetic field [4][11], on STT-current induced clocking [12] and on multiferroic structures [13]. In this work we propose an alternative solution [14], where the basic element is a simple magnet and not a multiferroic structure. Magnets are deposited on a piezoelectric layer (PZT) driven by two parallel electrodes buried inside or deposited on top of the PZT itself. After a background description in section II, the basic idea is described in Section III while in Section IV the circuit layout is shown. In Section V the performance of the proposed Magnetoelastic clock are shown and compared to the other NML technologies. The work presented in this paper provides three important contributions to the NML circuits theory (1). It demonstrates that the performance in terms of speed and power consumption are much better than other NML systems; (2) we show that, while from a pure theoretical point of view this solution has lower performance than a pure multiferroic structure, it is instead feasible with current technological processes and represents therefore a good trade off between performance and technological feasibility. Finally, (3) we reach the results through accurate simulations of realistic structures constrained by technological procedures currently available and ready to be experimentally demonstrated.

II. Background on NML clocking

Even the magnetic field induced by a Magnetic Force Microscope (MFM) tip, used to investigate the static magnetization configuration of the system, may be used to switch a single element, as already shown in [15]. However to propagate the information through the circuit a further mechanism is required. During the removal of the magnetic field, when magnets are switching, there can be errors due to the influence of external factors like thermal noise [16]. This is true also applying the so called adiabatic switching, that means a slow rise and fall time for the magnetic field. This problem originates when too many elements are cascaded, while when the number is limited the information safely propagates with a small error probability.

To solve this problem a multiphase clock system must be applied at the circuit (Figure 1.D) [11]. Three clock signals with a phase difference of 120 degrees are applied to different areas of the circuit, called clock zones. These areas are composed by a limited number of magnets. As shown in Figure 1.D, at every time instant when magnets of a clock zone are switching (SWITCH phase) magnets on their left are in the HOLD phase, they are in a stable state and act like an input for the switching magnets. Elements of the clock zone on the right are in the RESET state and have no influence on the switching magnets. At the next time step (Figure 1.D) the situation is repeated but the switching clock zone is the next in the sequence, therefore information propagates through the circuit avoiding errors. Ideally every clock zone must be wide exactly as one magnet. With this solution the error probability would be reduced at the minimum possible value and at the same time it would be possible to reach the maximum clock frequency [17]. The downside of this solution is that a precise spatial control is required to influence only one element and not its

neighbors. Moreover, the pipeline level of the circuit greatly increases and this can reduce the throughput in sequential circuits [18]. As a consequence, the number of elements for each clock zone must be carefully chosen considering speed and reliability constraints, but also technological and circuit architecture issues [19].

The clock frequency obtainable are in the range of 50MHz-500MHz [20][12][21], depending on the clocking technology chosen, so it is lower than the frequency obtainable with CMOS [22] or with emerging technologies based on molecular structures [23][24]. However, the main interest beyond Nano-Magnet Logic is the expected very low power consumption, lower than the expected power consumption of ultimate scaled CMOS transistors [25][26]. The power consumption is lower than CMOS if only the energy required to switch the magnets is considered. Nonetheless if the losses in the clock generation system are considered as well, this is no more true and most of the advantages of this technology are wiped out [19]. In [4] a current of 545mA in a copper wire of 1μm width is considered necessary to switch all the magnets, leading to a very high power consumption due to Joule losses. Moreover, using this approach the local control of a clock zone is difficult to reach, because the magnetic field of one clock zone influences also the neighbors clock zones [7]. To solve this problem new clocking technologies were studied. An STT-current induced clock was proposed as a suitable way to reset the magnets (Figure 1.B) [12][27]. In this NML implementation Magnetic Tunnel Junctions (MTJs) are used as basic cells. MTJs are multilayer structure composed by an insulator layer sandwiched between two magnetic layers. This is the same structure used in Magnetic RAM, and allows to reset every element with a current flowing "through" each element. The advantages of this approach are many: Much lower power consumption, built-in read/write system, perfect local control of each element and the possibility to use the well developed MRAM technology. Another solution recently proposed uses multiferroic [13] structures as base elements (Figure 1.C) [17][21]. The basic dots are composed by 40nm of piezoelectric material (PZT - lead zirconate titanate [28]) and a 10nm magnetic layer. Every element is then controlled by applying a voltage of few millivolt (mV). When the voltage is applied the strain of the magnetic layer, induced by the coupled piezoelectric material, makes the magnetization vector rotate toward the short side of the magnet, working as a reset mechanism. This system allows to reach the highest possible frequency with the lowest possible power consumption, with, at the same time, the possibility to use a voltage instead of a current to control the circuit.

While this approach is a very good solution for NML logic, that might allow in the future to exploit the full potential of NML logic, it presents two major problems that makes the fabrication of the circuit quite difficult. The aspect ratio of every element is very low, with a difference of two nanometers between the two sides. Since most of the properties of nano-magnets depend on their aspect ratio, changing it drastically implies a change on how the correspondent circuit works. With a so small difference between the shorter and the longer side of magnets, the presence of unavoidable process variations

can easily alter the magnets behavior, leading to improper magnets behavior. Moreover, a very precise local control on magnets is required, making the application of the electric field and the related electrodes fabrication quite complex, and currently almost unfeasible. The solution here discussed aims at a feasible structure, which unavoidably contraints the results, but that still has remarkable performance and potentials for improvements.

III. MAGNETOELASTIC CLOCK SYSTEM

A. Structure description

The basic idea is shown in Figure 2. A magnetic thin film is deposited above a piezoelectric substrate and it is patterned through lithography (Figure 2.A). When an electric field is applied to the substrate, the piezoelectric material increases its length. If the piezoelectric figure of merit is such that the resulting strain is large enough to induce a stress on the ferromagnetic layer which is above the film mechanical stiffness, a strain is produced in the nanomagnet too. Of course this depends on both materials choice (properties) and on device geometry, as shown in detail further in the article. The induced stress-anisotropy causes the magnetization vector to rotate along the direction of the applied strain (Figure 2.B) This is the direct mapping of the clock principle that drives NanoMagnet Logic.
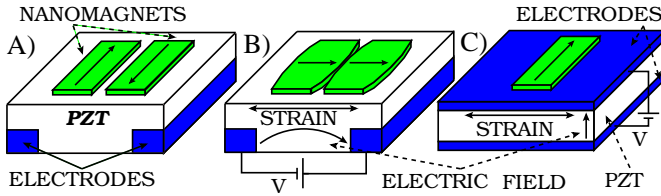

Fig. 2. Magnetoelastic clock for NanoMagnet Logic. A) No voltage applied. B) Voltage applied to the PZT substrate. The strain induced in the nanomagnets change their magnetization. C) First demonstration of a magnet switched with the strain induced by a piezoelectric layer, with electrodes placed on top and on the bottom of the PZT [29].

It is a rather simple idea that was already demonstrated in a simplified form in [29]. In [29] an electric field was applied using two parallel electrodes placed on top and on the bottom of a piezoelectric (PZT - Lead Zirconate Titanate) substrate (Figure 2.C). Relatively big (380x150 nm^2) Nickel magnets where successfully switched by applying a small voltage (1.5V). Table I shows a comparison among the more common piezoelectric materials, PZT, BT (Barium Titanate), ZnO (Zinc Oxide) and PVDF (polyvinylidenfluoride). PZT is clearly the best choice for this kind of applications, as discussed in the following.

When applying the same concept of [29] to NML logic some issues arise. Electrodes placed on top of the PZT substrate are difficult to contact, because the surface of the PZT must be patterned with nanomagnets. Moreover with this configuration the electric field is perpendicularly applied, while the strain is parallel to the PZT surface. In this way the strain and the electric field are coupled through the d_{31} coefficient (d coefficients, normally expressed in pm/V, describe the coupling between strain and electric field in the stress-charge tensor). PZT d_{31}

TABLE I
COMPARISON BETWEEN PIEZOELECTRIC THIN FILMS. D31 AND D33 ARE THE TWO MAIN PIEZOELECTRIC COEFFICIENTS. Ef_{MAX} IS DIELECTRIC STRENGTH AND ϵ_r IS THE DIELECTRIC CONSTANT.

	d_{31} (pm/V)	d_{33} (pm/V)	Ef_{MAX} (MV/m)	ϵ_r
PZT	-30 to -80	50 to 150	>50	300 to 1300
BT	-33	82	2	1250 to 10000
ZnO	0.26	5.9	25 to 40	10.9
PVDF	23	-33	5	12

is much lower than the d_{33} coefficient, that applies when the voltage and the strain lie along the same direction. The solution that we propose comprises electrodes placed under the piezoelectric layer (Figure 2). As a consequence electric field and strain lie along the same direction and they are therefore coupled through the d_{33} coefficient. The remarkable consequence is that a lower voltage is required to generate the same strain and the power consumption is reduced. Moreover with this configuration electrodes can be contacted from the bottom, without interfering with nanomagnets that are placed on top of the PZT layer and resulting in a great process simplification. Further details on the structure are given in Section IV.

B. Choice of magnetic material and magnet sizes

In order to choose the proper magnetic material and the nanomagnets geometry the maximum and minimum stress that can be applied must be accurately evaluated. To evaluate the maximum stress first of all the maximum strain due to dielectric rigidity must be considered as in equation (1):

$$\xi_{MAX\_RIG} = Ef_{MAX} \cdot d \qquad (1)$$

where $Ef_{MAX} = 20MV/m$ is the maximum electric field that the PZT layer can tolerate without electrical breakdown, and $d = d_{33} = 150pm/V$ is longitudinal piezoelectric coefficient that relates the strain induced with the applied field. The previous value (ξ_{MAX_RIG}) must be compared with the maximum strain achievable in the piezoelectric layer due to structural limitations (ξ_{MAX_STRUCT}), as in equation (2)

$$\xi_{MAX} = min(\xi_{MAX\_RIG}, \xi_{MAX\_STRUCT}) \qquad (2)$$

where $\xi_{MAX\_STRUCT} = 500 \cdot 10^{-6}$ [30]. Between these two components the more constraining in the PZT is the maximum strain due to the dielectric rigidity. Once the maximum strain (ξ_{MAX}) is known it is possible to evaluate the maximum stress applicable to the magnets (σ_{MAX_PIEZO}), making the assumption that the former are thin enough to make the PZT strain totally transferred on them (equation (3)):

$$\sigma_{MAX\_PIEZO} = Y_{Magnet} \cdot \xi_{MAX} \qquad (3)$$

where Y_{Magnet} is the Young modulus of the magnetic material chosen. But we also need to consider the fracture stress of the magnets, which depends on the selected material. Consequently, the maximum stress that can be transferred to the magnets is indicated (equation (4)):

$$\sigma_{MAX} = min(\sigma_{MAX\_STRUCT}, \sigma_{MAX\_PIEZO}) \qquad (4)$$
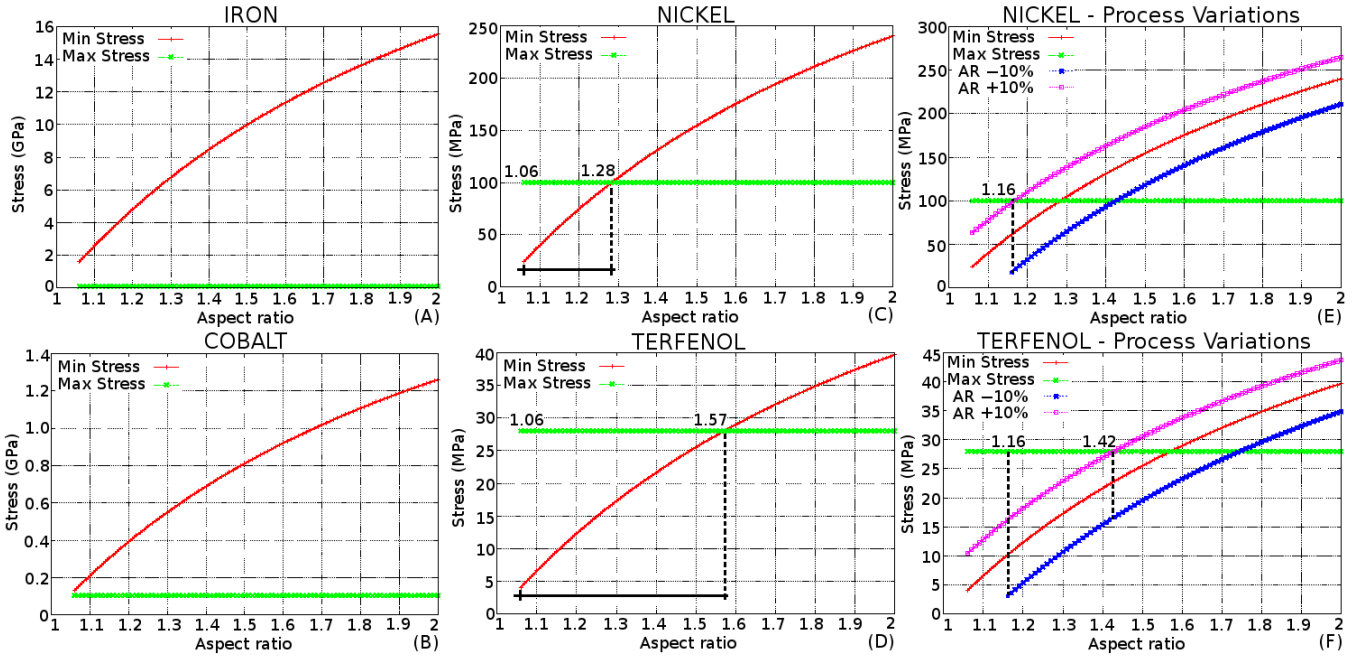
Fig. 3. Comparison between the minimum required stress and the maximum applicable stress for different magnetic materials. A) Iron. B) Cobalt. C) Nickel. D) Terfenol. E) Nickel considering a process variation of +/- 10%. F) Terfenol considering a process variation of +/- 10%.

where σ_{MAX_STRUCT} is the maximum mechanical stress that can be applied to the magnets. The minimum stress is related to the height of the energy barrier between the two stable states, which depends on magnetic shape anisotropy. Shape anisotropy is related to magnets shape: If magnets have an aspect ratio different from 1, at the equilibrium magnetization will lie along the longer side of the magnets. In this case the height of the energy barrier between the two stable states depends on the aspect ratio of the magnets. The minimum applicable stress is therefore the stress that generates a stress anisotropy at least equal to the shape anisotropy [17]:

$$\frac{1}{2}\mu_0 N_d M_s^2 V = \frac{3}{2}\lambda_s \sigma V \qquad (5)$$

where N_d is the demagnetization factor [31], M_s is the saturation magnetization, V is the volume and λ_s is the magnetostrictive coefficient. The minimum applicable stress is therefore:

$$\sigma_{MIN} = \frac{\mu_0 N_d M_s^2}{3\lambda_s} \qquad (6)$$

TABLE II
MAGNETIC MATERIALS COMPARISON. M_S IS THE SATURATION MAGNETIZATION, $\lambda_1 00$ AND $\lambda_1 11$ ARE THE MAGNETOSTRICTIVE COEFFICIENTS, WHILE Y IS THE YOUNG MODULUS AND σ (ABBREVATION FORM OF σ_{MAX_STRUCT}) IS THE FRACTURE STRESS.

Magnetic material	Ms $(10^6$ A/m)	λ_{100} $(\cdot 10^{-6})$	λ_{111} $(\cdot 10^{-6})$	Y (GPa)	σ (MPa)
Iron	1.71	-7	-7	211	540
Cobalt	1.45	-62	-62	209	225
Nickel	0.49	-46	-24	214	100
Terfenol	0.8	600	600	80	28

NML logic requires the use of single domain nanomagnets, that means with sides shorter than 100nm for typical soft ferromagnets. In literature magnets are normally 50x100 nm^2 [32] or 60x90 nm^2 [4]. We choose therefore a shorter side of

the magnets of 50nm with a thickness of 10nm. The magnets aspect ratio determines the value of the shape anisotropy, i.e. the height of the energy barrier. To have a reasonably small value of error probability ($p < e^{-30} \approx 10^{-13}$), the energy barrier at room temperature must be at least

$$\Delta E = 30 K_b T \approx 1.24 \cdot 10^{-19} J \qquad (7)$$

This means that the value of the shape anisotropy must be at least equal to ΔE

$$\frac{1}{2}\mu_0 N_d M_s^2 V = \Delta E \qquad (8)$$

From this equation it is possible to evaluate the value of N_d and therefore the minimum value of aspect ratio. The minimum aspect ratio is 1.06, that means minimum sizes for the magnets of 50x53x10 nm^3. Smaller magnets will have an energy barrier lower than $30 K_b T$, and therefore the error probability will be too high. To choose a suitable magnetic material we have evaluated the minimum stress necessary to reset the magnets starting from an aspect ratio of 1.06 to 2, comparing this value to the maximum applicable stress. Table II shows the main characteristics of some magnetic materials.

Results of the analysis are shown in Figure 3. For most classical magnetic materials, like Iron or Cobalt, there is no range in which the circuit can work properly. Figure 3.A shows the results obtained for Iron, the minimum required stress, evaluated from equation 6, is always bigger than the maximum applicable stress. This is caused because Iron is a material with negligible magnetostriction. The same thing happens for Cobalt as shown in 3.B. Cobalt has higher magnetostriction than Iron, but its saturation magnetization is much higher, as shown in Table II. As a consequence Cobalt cannot be used for this application as well as Iron. Figure 3.C shows the results obtained for Nickel. Results show a range in which the device can operate, from 1.06 to 1.28 aspect ratio (53-64

nm). Things change dramatically if a high magnetostrictive material, like the Terfenol, an alloy of Iron and Dysprosium ($Tb_xDy_{1-x}Fe_2$) is considered (Figure 3.D). In this case the working range increases a lot, from 1.06 to 1.57 aspect ratio (53-78.5 nm). Moreover the required stress is lower than the required stress for the Nickel (100 MPa for Nickel, 28 MPa for Terfenol).

Although both Nickel and Terfenol can be suitable targets for this technology, the limited operative range of Nickel can be a problem if process variations are considered. For example considering a process variation of +/-10% different results are obtained, as shown in Figure 3.E. The central curve represents the minimum stress in normal conditions, evaluated from equation 6. The lower and upper curves represent the minimum required stress, evaluated from equation 6 considering a variation of -10% (lower curve) and +10% (higher curve) of the shorter magnets side. The value of stress to be applied to the circuit must be chosen according to the central curve, which represents how the minimum stress varies with the aspect ratio, in normal conditions. If a random process variation will cause a random variation in one or more magnets aspect ratio, the operating points will shift up or down. The consequence is that another value of stress, different from the design parameters, will be required. If the working point shifts outside the limits, magnets will not be reset properly. As a consequence the aspect ratio must be chosen in a way that, in case of random shifting due to process variations, it still falls in the acceptable range (between 0 and the maximum applicable stress). Figure 3.E shows the working range of Nickel considering process variations of +/-10%. There is only one point that lies in the operative range, correspondent to an aspect ratio of 1.16. A negative variation due to the process increases the minimum aspect ratio. This can be understood by equation (8). A negative aspect ratio reduces the magnet volume. Since the value of ΔE is constant, the demagnetization factor N_d increases, and so does the correspondent value of minimum aspect ratio [31]. This means that Nickel is very sensitive to process variations, it tolerates variations lower than 10%. Figure 3.F shows the working range for Terfenol instead. The minimum value for the aspect ratio becomes 1.16 while the maximum becomes 1.42. This means that Terfenol has a very good working range and can tolerate process variations even near +/-20%. We can conclude from these analyses that high magnetostriction materials, like Terfenol, are the best candidates for this application.

As a consequence, then, in this work we choose to use nanomagnets made of Terfenol, with sizes of 50x65x10 nm^3. Comparing this geometry with the one proposed in [17] the difference between the smaller and bigger magnet is higher (15nm instead of 2nm) and magnets are simple single layer structures. This means that they are easier to fabricate and also tolerant to process variations.

IV. CIRCUIT LAYOUT

The layout of the circuit must take into account two important problems: Signal propagation and fabrication processes.

A. The process

The solution that we propose is shown in Figure 4.A. Parallel electrodes are buried under a PZT layer, and nanomagnets are deposited directly on top of it. This solution is technology-friendly because it is compatible with CMOS planar technology and, supposing to have a high end resolution lithographic system, can be fabricated. After the deposition of metal to create the electrodes, the PZT is deposited on top of them either by means of a sol-gel process or by means of sputtering. The processes used for PZT deposition create a layer with a very small roughness (less than 3nm). Electrodes can be fabricated with platinum or copper, however in case of copper a seed-layer of Titanium Oxide (TiO_2) must be used. Nanomagnets can be fabricated by depositing a thin film of magnetic material on top of it and then patterning the film using lithography. The small roughness of the PZT substrate has no influence on the magnets, neither in the magnetic material deposition and in the following lithographic phase, neither on the magnetic properties of the deposited material. The fabrication process is relatively simple but the problem arising is how the electric field will be distributed in the piezoelectric layer. Figure 4.E shows a Comsol Multiphysics [33] simulation of the structure, which enlights the distribution of the electric field. Electrodes are 50nm width while the distance among them is 250nm. According to the ITRS roadmap the Metal 1 pitch, the center-to-center distance between two neighbor metal lines in case of the lowest interconnection level, is 54nm for the 2013 year. This is a value compatible with the requirement of this clock solution and it also leaves space for further scaling. The applied voltage is 1V and an electric field of 3-4MV/m is generated almost uniformly between the two electrodes. In correspondence of the electrodes the electric field abruptly decreases and reaches a value of about 2MV/m near the borders. The strain of the PZT is proportional to the electric field, so it is clear that the strain will be smaller near the areas corresponding to the electrodes. However, due to mechanical continuity, the higher strain of the central area will induce a strain also in the area exactly above the electrodes, where the electric field has a very low value. This issue could be improved reducing the distance between the electrodes and the PZT surface. However, from the technological point of view, it is more complex to fabricate. From the results of Figure 4.C the strain can be approximated as uniformly applied in the area between the two electrodes. The consequence is that, to obtain working circuits, magnets must not be placed in the area correspondent to the electrodes. An alternative structure is shown in Figure 4.B, where electrodes are placed on top of PZT. The distribution of the electric field is similar to the previous case (Figure 4.F): Also in this case the electric field varies in the range of 3-4MV/m with an applied voltage of 1V. The main problem of the previous solution (Figure 4.A) is that PZT is fabricated on top of the electrodes (made of Copper). Nonetheless PZT requires high temperature (600 Celsius degrees) processes, which can oxidize the Copper. Moreover, a seed-layer is required to attach the PZT on the electrodes. Platinum can be used instead of Copper but is expensive. This second solution has the advantage that the PZT
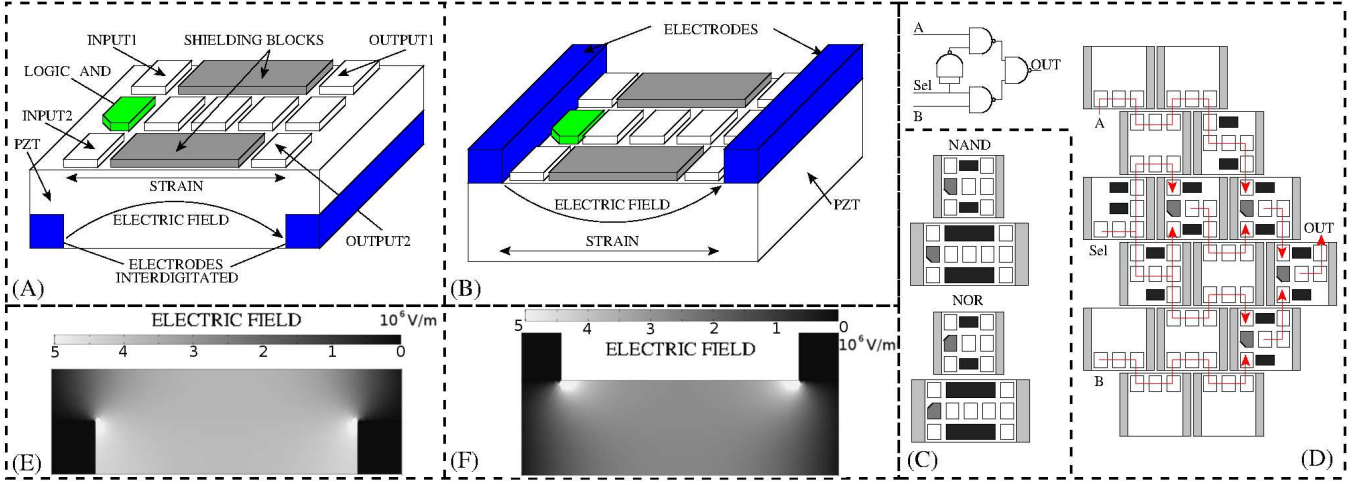
Fig. 4. Magnetoelastic clock system. A) Proposed structure. Parallel electrodes buried under the PZT layer generate the electric field. The strain transfers to the magnets that are reset. Input and output propagate vertically from each corner. Shielding blocks are used to avoid propagation errors. B) Alternative structure: Electrodes are placed on top of the PZT layer. C) Universal NAND/NOR gates. Every gate is high 3 magnets and with a variable width of 3 or 5 magnets. D) Circuit design example: 2 to 1 multiplexer. Each row is composed by many clock zones of area 3x3 or 3x5 magnets. Alternate rows are shifted to allows signal propagation. E) Comsol Multiphysics simulation of the structure with buried electrodes. The electric field (and as a consequence the strain) is almost uniform between the two electrodes. F) Comsol Multiphysics simulation of the structure with electrodes on top of the PZT.

is fabricated before the electrodes. Circuits structure remains the same, because even in this case magnets cannot be placed in the area of the electrodes. Another advantage of placing electrodes on top of the PZT layer is that they can be contacted from above, making the fabrication of wires for the clock distribution network easier. Additional layers can be used to route clock wires, similarly to what happens in CMOS chips.

B. Logic gate organization

We therefore base our design on 2 input AND/OR gates [6], as shown in Figure 4.A, B. AND/OR gates are made by three magnets, the shape of the central magnet is changed to obtain the desired logic function, the corner is cut so that the magnet get a preferred direction for the magnetization. The advantage of this solution is that inputs come from vertical directions (up or down), where there are no electrodes. Another point is that in NML logic the horizontal coupling is antiferromagnetic, i.e. every magnet has the inverted value of its predecessor. So, if the number of magnets in the clock zone (the zone between two electrodes) is odd, the signal is inverted. Placing therefore an AND/OR gate in a clock zone with a width equal to an odd number of elements generates a universal NAND/NOR gate that can be used as basic block to build any circuit. Ideally the width of the clock zone should be equal to one magnet to obtain the maximum possible clock frequency, as shown in [17]. However this approach has two disadvantages: It increases the latency of the circuit and it makes the fabrication of the structure and the signal propagation almost impossible. Increasing the latency of the circuit reduces the throughput in presence of sequential circuits [34]. Moreover, the distance between the electrodes will be smaller and the whole structure more difficult to fabricate. Also, since magnets cannot be placed over the area of the electrodes, with a width of one magnets there is not enough space to propagate the output signal of the logic gate. We therefore choose a width of the gate of 3 or 5 magnets, as shown in Figure 4.C.

C. Signal propagation in gates

Inputs come from up-left and bottom-left corners, output of the AND/OR gate is propagated to the up-right and down-right corners. In this way signals can propagate to the others parts of the circuit avoiding the area of the electrodes. Helper/shielding blocks [35] are used to help the signal propagation and to reduce the error probability. With a width of 5 magnets the critical path (the maximum number of magnets between input and output) is higher, 7 magnets instead of 5 magnets in case of a width equal to 3 elements. Since the clock frequency depends on the critical path, with a width of 5 magnets the clock frequency will be lower but the structure is bigger and easier to fabricate. Sizes bigger than these are not possible, because, not only the clock frequency would be much lower, but the length of the critical path would be too big, increasing the error probability during magnets switching.

D. Complete layout

A circuit example, a 2to1 multiplexer, is shown in Figure 4.D. Clock zones are made by mechanically isolated cells of 3x5 or 3x3 magnets. Every cell is an independently actuated clock zone, where logic gates or interconnection wires can be placed. To create this layout it is possible to pattern the PZT substrate, removing the PZT (Figure 5) [36][37]. It is possible to dig through the PZT until the bottom, or to remove only a part of the PZT to mechanically isolate the areas. In both solutions a perfect mechanical isolation is obtained, but probably the complete removal of the PZT will reduce parasitic parameters. Clearly, the resolution of the optical lithography must be quite high to remove only a small area of the piezoelectric layer. Theoretically, it would be sufficient to remove few nanometers between the clock zones, but it is quite difficult to obtain this result using lithographic processes currently available.
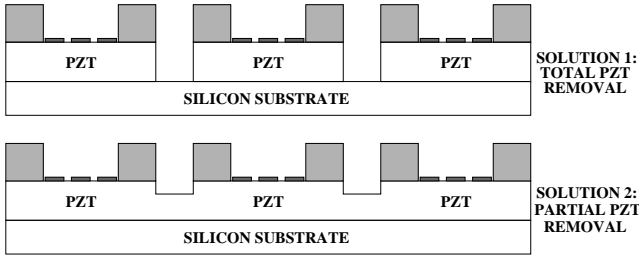
Fig. 5. PZT can be patterned to obtain mechanically isolated cells. Two solutions are possible: Complete or partial removal of the PZT.

E. Overall signal propagation

Signal propagation happens through the corner of each clock zone, to avoid the area of the electrodes. To allow this, there must be a shifting in each row of clock zones, as can be seen from Figure 4.D. With this layout the width of the clock zone must therefore be chosen according to the size of the electrodes. With 3 magnets zone, electrodes must have an ideal width of 30-40 nm, while in 5 magnets clock zones electrodes can be approximately 70-100 nm wide, a size that can be reached in scaled CMOS technology. Since this approach is based on universal NAND/NOR gates, in principle every kind of circuit can be implemented, moreover the circuit layout is quite regular, and this always helps the technological fabrication as well as the circuit physical design.

F. Technology scaling

One of the advantages of this clock solution is that it is feasible with available technological processes. The structure sizes reflect this choice. However, like in CMOS, scaling can reduce the circuit area and improve power consumption as discussed in Section V. The minimum sizes of the NAND gate however cannot be changed. Every NAND gate must be at least 3x3 magnets, but it is possible to reduce the magnet sizes. The energy barrier must be higher than $30K_bT$ to have a reasonably small value of error probability. This pose a limit to the minimum values of magnet sizes. As shown in [7] magnets can be as smaller as 15x30x5 nm^3, and still have an energy barrier of $30K_bT$. Thus, provided to have lithographic processes with high enough resolution, it is possible to further scale magnets reducing their size to half the actual value, reducing consequently the circuit area by 4 times.

V. PERFORMANCE ANALYSIS

To verify the effectiveness of the solution proposed in this work we have accurately estimated its performance both in terms of timing and of power consumption. Figure 6 shows the timing characteristics obtained through Magpar [38] simulations. Magpar is a finite element simulator that allows the evaluation of the magnetoelastic effect applied to the dynamics of a magnetic circuit.

A. Timing

In Figure 6.A the time required to reset the magnets is indicated. About 1 ns is necessary to completely reset the magnets. Figure 6.B shows that also the switching time

(T_{SWITCH}) of every magnet is near 1 ns. The clock frequency can therefore be estimated starting from these data. The clock period must last enough to allow the reset of the magnets and their successive realignment. So, as a first approximation, the minimum clock period can be calculated as in equation 9:

$$T_{ck} = T_{RESET} + N * T_{SWITCH} \qquad (9)$$

where N is the number of magnets in the critical path (5 considering a 3x3 NAND, 7 considering a 5x5 NAND). However the situation is more complex, because in a chain of magnets one element starts to switch before its neighbor has reached a stable state. So the clock period is not directly the sum of N switching times. As a consequence the maximum clock frequency obtainable is around 200MHz for 3x3 NAND/NOR gates and 150MHz for 3x5 NAND/NOR gates. The frequency is lower than the one obtained in [17], but this is due to the higher number of elements in the critical path.
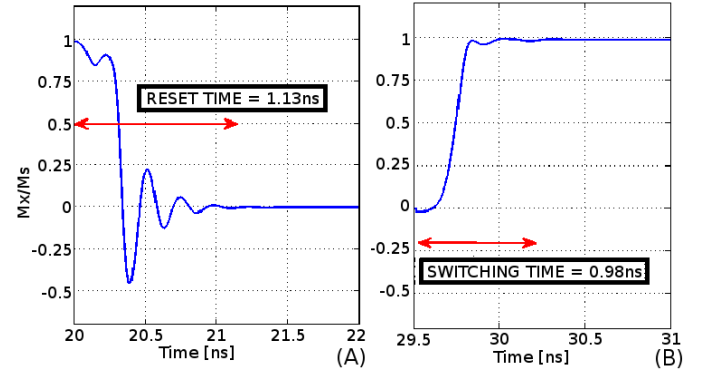

Fig. 6. A) Nanomagnets RESET time. B) Nanomagnets SWITCH time. Both times are in the order of 1ns.

B. Power consumption

It is worth remarking, however, that speed is not the major advantage of NML logic. This technology is particularly interesting for the expected low power consumption obtainable. There are two main sources of power consumption: The energy required to force the magnets in the RESET state and the losses in the clock generation system. As explained in Section III the energy required to RESET a magnet is about $180K_bT$, which correspond to 0.85aJ. The origin of this lies in the fact that an abrupt switching was applied to achieve the maximum circuit speed. Using an adiabatic switching (i.e. very slow rise and fall time for the clock signals, in the order of many nanoseconds) this energy can be reduced to $30K_bT$, greatly reducing the obtainable circuit speed.

In NML circuits the major source of power consumption are the losses in the clock generation system. In the magnetoelestic clock case, power consumption depends mainly on the energy required to charge the parasitic PZT capacitance. With this purpose we show the equivalent circuit of a NAND/NOR gate is shown in Figure 7.A.

The capacitor (C_{pzt}) represents the parasitic capacitance of the PZT substrate. Since the PZT is an insulator, it has an considerable parasitic resistance (R_{pzt}). This resistance is used to evaluate the leakage current between the two electrodes of the capacitor. The resistance value is around $10^{18}\Omega$, so the
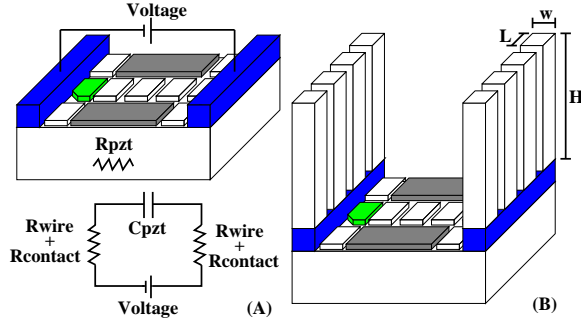
Fig. 7. A) NAND/NOR equivalent circuit. B) Possible example of contact via for electrodes.

leakage current can be assumed equal to 0. The capacitor is connected to the voltage source through resistances that represent the on-chip interconnections. The exact evaluation of these resistances is not possible at this development stage, since we do not know the complete on-chip layout of interconnection wires. However, it can be assumed that the most important contribution to the resistance is due to VIAs used for the direct connection with the electrodes. This assumption is based on the fact that VIAs have the smallest section and the higher resistance, while global interconnections have normally a much wider section and therefore much smaller resistance. A possible example of interconnection made using an array of VIAs is shown in Figure 7.B. Assuming a VIA made of copper with a width (W) of 40nm, a length (L) of 40nm and an height (H) of $1\mu m$, the obtained resistance is 10Ω. In case 4 VIAs are connected in parallel, the whole resistance is divided by 4, leading to a value of 2.5Ω.

When a capacitor is charged, part of the energy is dissipated on the parasitic resistance due to the joule effect. This energy can be evaluated as shown in the equation (10)

$$E = \int_{t1}^{t2} \frac{V^2}{R} \cdot (e^{\frac{-t}{RC_{pzt}}})^2 dt \qquad (10)$$

where $t1$ and $t2$ are respectively the beginning and the end of the time period considered, V is the applied voltage, C_{pzt} the capacitance and R the interconnection wires resistance. The applied voltage can be evaluated as equation (11)

$$V = \frac{w_{NAND} \cdot \sigma}{Y \cdot d_{33}} \qquad (11)$$

where σ is the applied stress, Y is the Young modulus of the magnetic material and d_{33} is the piezoelectric coefficient of the PZT. The capacitance can be approximately evaluated as equation (12)

$$C_{pzt} = \frac{\epsilon_0 \cdot \epsilon_r \cdot t_{PZT} \cdot h_{NAND}}{w_{NAND}} \qquad (12)$$

where ϵ_r is the relative dielectric constant of the PZT, t_{PZT} is the thickness of the PZT and h_{NAND} and w_{NAND} are the height and the width of the NAND gate. Considering a NAND/NOR gate with a size of 3x3 Terfenol magnets and a PZT thickness of 40nm, the voltage is 0.368V while the capacitance is 0.678fF. It is worth noting that the ϵ_r of the PZT is quite high, thus further advantages are expected by studying other materials with similar propertis but smaller dielectric constant. The circuit time constant τ, given by the product

RC_{pzt}, rules the circuit dynamic behavior. The resulting value of τ is around few fs (10^{-15}s), so each NAND/NOR gate can theoretically work at THz. However, the magnets dynamic is much slower and is in the order of nanoseconds (Figure 6), so it limits the overall circuit speed.

When the time constant value is much smaller than the integration period ($t2 - t1$), equation (10) becomes the well known equation (13)

$$E_{clock} = \frac{1}{2} \cdot C_{pzt} \cdot V^2 \qquad (13)$$

which tells us that in the charging process half of the energy supplied is dissipated on the resistance. Similarly to the CMOS case the other half energy is dissipated on the resistance in the discharging process, and the total energy dissipation is then given by equation (14)

$$E_{clock} = C_{pzt} \cdot V^2 \qquad (14)$$

Two important facts must be observed: First, this is an energy, so its independent from the value of frequency used; second, the energy value is totally independent from the resistance value, so it is not necessary to evaluate the parasitic resistance of interconnections. To be fair, the choice of properly setting up a RLC resonant circuit could help reducing the energy consumption. However, here the aim is to analyze the worst case scenario, so we assume that all the energy is dissipated on the resistance. In this case the energy dissipated in the parasitic resistance is therefore 91 aJ, while 6aJ are required to RESET magnets, leading to a total power consumption of 97aJ for a NAND/NOR gate.

Scaling magnets size can reduce the global power consumption of the circuit. With magnets of sizes currently reachable, the energy barrier is $180K_bT$. Reducing for example their sizes to 15x30x5 nm³ causes a reduction of the energy barrier to $30K_bT$. Smaller magnets means also smaller clock zones. With smaller clock zones a lower voltage can be used, reducing therefore power losses due to the RC circuit dynamic.

TABLE III
POWER COMPARISON AMONG THE MAIN NML IMPLEMENTATIONS CONSIDERING BOTH NANOMAGNETS SWITCHING AND CLOCK LOSSES.

		Energy (fJ)	Clock (MHz)
a	Magnetic Field	62	50-100
b	STT-current	11	100-200
c	Multiferroic	0.004	500
d	**Magnetoelastic**	**0.097**	**200**
e	CMOS 28nm	0.857	~200MHz
f	CMOS 28nm	1.304	~1GHz

Clock solutions at a glance. Finally a comparison between the different clock systems is mandatory. Table III shows the total energy consumption and the obtainable frequencies for a NAND gate based on a NML logic implementations. In case of magnetic field clocked NML an adiabatic switching is considered, therefore the energy required to reset magnets is taken equal to $30K_bT$ for each magnet. The energy losses due to Joule effect was also estimated. The wire has a section of about 400x400nm and a length of about 200nm, it is made of copper and the current value is 2mA (extrapolated from [4]). This leads to an energy consumption of 62fJ for a NAND

gate (table III.a). The frequency achievable, due to the use of adiabatic switching, is in the range of 50-100MHz [20]. For STT-current induced clock data are obtained from Das and co-workers [12]. An energy of 1,6fJ is necessary to reset the magnets that gives a total of 11fJ for a NAND gate (table III.b). This system is much better than the magnetic-field based clock. Frequencies obtainable are among the highest in the range of 100-200MHz [27]. Considering instead multiferroic logic, data shown in [17] indicates a total energy required to operate a NAND gate of about 4 aJ (table III.c), at least 3-orders better than the current based approaches. The frequencies is also relatively high, at about 500MHz. Finally, In our magnetoelastic case we obtain an energy consumption of 97aJ and a maximum frequency of 200MHz (table III.d). Although these values are far better than the current based approaches, a pure multiferroic logic still appears to show better performance, at least in ideal conditions. The reason is easy to understand as the NAND gate in this case is made by 7 magnets, while a pure multiferroic approach requires just 3 magnets. However, one important fact can be underlined: The technique we propose represents an easier and more feasible technological approach and circuits could be already fabricated with high resolution techniques. In this work we are considering a realistic and feasible layout and a realistic process, differently from the previous multiferroic study.

A final interesting outcome can be observed from table III lines e and f, where the energy consumption of a 28nm CMOS NAND gate is shown for the same frequency used for the magnetic case (200MHz) and for a typical frequency in 28nm based circuits (1GHz). Data in the CMOS case are obtained using an industrial technology. The CMOS NAND has an input capacitance of around 0.55fF, which is slightly smaller than our capacitance, but the supply voltage is much bigger, around 0.9V. As a consequence the dynamic power consumption is 12nW at 200MHz, i.e. an energy of 117aJ. In CMOS technology the impact of leakage currents must be considered as well: in the NAND case the energy due to leakage assumes a value around 740aJ. If adiabatic techniques are used with CMOS transistors the dynamic energy consumption can be reduced, while the leakage energy remains big. Further transistors scaling does not help because, while the dynamic energy consumption is reduced, leakage energy consumption is predicted to increase. It is than clear that NML circuits, in particular considering the magnetoelastic clock, hold a considerable advantage in terms of power consumption, which is one order of magnitude lower.

VI. Conclusions

We have proposed a magnetoelastic clock system for Nano-Magnet Logic that uses a piezoelectric layer to strain the magnets and change their magnetization. We demonstrated that power consumption is 100 times smaller than current-based clock systems and also the clock frequency obtainable is higher. This clock solutions has also a lower power consumption compared to scaled CMOS transistors. Mostly important, this solution was designed keeping in mind the technological processes and their current limitations. Actually our solution

does not reach the performance of a full multiferroic system in theoretical conditions, but shows remarkable improvements being feasible with current technological limitations, marking then a difference with respect to previous proposed solutions. Moreover the structure shows a good tolerance to process variations, which is always a remarkably important point for the fabrication of a real working circuit.

This solution soundly enhances the knowledge on NML logic, addressing its main issues, the high power consumption of the clock generation system and the necessity to have a local control on a limited circuit area. At the same time it allows to make a huge step toward the fabrication of a complex magnetic circuits. Our efforts are now directed to the experimental demonstration of the results shown here.

VII. Acknoledgements

References

[1] A. Imre, L. Ji, G. Csaba, A.O. Orlov, G.H. Bernstein, and W. Porod. Magnetic Logic Devices Based on Field-Coupled Nanomagnets. *2005 International Semiconductor Device Research Symposium*, page 25, December 2005.

[2] J. Pulecio and S. Bhanja. Magnetic cellular automata coplanar cross wire systems. *Journal Applied Physics*, 107(3), 2010.

[3] D.K. Karunaratne and S. Bhanja. Study of single layer and multilayer nano-magnetic logic architectures. *J. Appl. Phys*, 111, 2012.

[4] M. Niemier and al. Nanomagnet logic: progress toward system-level integration. *J. Phys.: Condens. Matter*, 23:34, November 2011.

[5] A. Chiolerio, P. Allia, and M. Graziano. Magnetic dipolar coupling and collective effects for binary information codification in cost-effective logic devices. *Journal of Magnetism and Magnetic Materials*, (324):3006–3012, 2012.

[6] M.T. Niemier, E. Varga, G.H. Bernstein, W. Porod, M.T. Alam, A. Dingler, A. Orlov, and X.S. Hu. Shape Engineering for Controlled Switching With Nanomagnet Logic. *IEEE Transactions on Nanotechnology*, 11(2):220–230, March 2012.

[7] M. Vacca, M. Graziano, and M. Zamboni. Majority Voter Full Characterization for Nanomagnet Logic Circuits. *IEEE T. on Nanotechnology*, 11(5):940–947, September 2012.

[8] S. Bhanja, M. Ottavi, F. Lombardi, and S. Pontarelli. QCA circuits for robust coplanar crossing. *Journal of Electronic Testing*, 23(2):193–210, 2007.

[9] M. Awais, M. Vacca, M. Graziano, and G. Masera. Quantum dot Cellular Automata Check Node Implementation for LDPC Decoders. *IEEE Transaction on Nanotechnology*, 12(3):368–377, 2013.

[10] M.T. Alam, M.J. Siddiq, G.H. Bernstein, M.T. Niemier, W. Porod, and X.S. Hu. On-chip Clocking for Nanomagnet Logic Devices. *IEEE Transaction on Nanotechnology*, 2009.

[11] M. Graziano, A. Chiolerio, and M. Zamboni. A Technology Aware Magnetic QCA NCL-HDL Architecture. pages 763–766, Genova, Italy, 2009. IEEE.

[12] J. Das, S.M. Alam, and S. Bhanja. Low Power Magnetic Quantum Cellular Automata Realization Using Magnetic Multi-Layer Structures. *J. on Emerging and Selected Topics in Circuits and Systems*, 1(3):267–276, September 2011.

[13] M. Fiebig. Revival of the magnetoelectric effect . *Journal of Physics D: Applied Physics*, (38):123–152, 2005.

[14] M. Vacca, M. Graziano, A. Chiolerio, A. Lamberti, M. Laurenti, D. Balma, E. Enrico, F. Celegato, P. Tiberto, and M. Zamboni. Electric clock for NanoMagnet Logic Circuits . *In: Anderson, N.G., Bhanja, S. (eds.), Field-Coupled Nanocomputing: Paradigms, Progress, and Perspectives. LNCS, Springer, Heidelberg.*, vol. 8280, 2014.

[15] A. Chiolerio, P. Martino, F. Celegato, S. Giurdanella, and P. Allia. Enhancement and correlation of MFM images: effect of the tip on the magnetic configuration of patterned Co thin films. *IEEE Transactions on Magnetics*, 46(2):195–198, 2010.

[16] G. Csaba and W. Porod. Behavior of Nanomagnet Logic in the Presence of Thermal Noise. In *International Workshop on Computational Electronics*, pages 1–4, Pisa, Italy, 2010. IEEE.

[17] M. S. Fashami, J. Atulasimha, and S. Bandyopadhyay. Magnetization Dynamics, Throughput and Energy Dissipation in a Universal Multiferroic Nanomagnetic Logic Gate with Fan-in and Fan-out. *Nanotechnology*, 23(10), February 2012.

[18] M. Graziano, M. Vacca, D. Blua, and M. Zamboni. Asynchrony in Quantum-Dot Cellular Automata Nanocomputation: Elixir or Poison? *IEEE Design & Test of Computers*, 28(5):72–83, September 2011.

[19] M. Vacca, M. Graziano, and M. Zamboni. Nanomagnetic Logic Microprocessor: Hierarchical Power Model. *IEEE Transactions on VLSI Systems*, 21(8):1410–1420, August 2012.

[20] N. Rizos, M. Omar, P. Lugli, G. Csaba, M. Becerer, and D. Schmitt-Landsiedel. Clocking Schemes for Field Coupled Devices from Magnetic Multilayers. In *International Workshop on Computational Electronics*, pages 1–4, Beijin, China, 2009. IEEE.

[21] J. Atulasimha and S. Bandyopadhyay. Hybrid spintronic/straintronics: A super energy efficient computing scheme based on interacting multiferroic nanomagnets . *2012 12th IEEE International Conference on Nanotechnology*, August 2012.

[22] A. Pulimeno, M. Graziano, and G. Piccinini. UDSM Trends Comparison: From Technology Roadmap to UltraSparc Niagara2. *IEEE Transactions on VLSI systems*, 20(7), July 2012.

[23] A. Pulimeno, M. Graziano, D. Demarchi, and G. Piccinini. Towards a molecular QCA wire: simulation of write-in and read-out systems. *Solid State Electronics*, 77:101–107, 2012.

[24] A. Pulimeno, M. Graziano, A. Saginario, V. Cauda, D. Demarchi, and G. Piccinini. Bis-ferrocene molecular QCA wire: ab-initio simulations of fabrication driven fault tolerance. *IEEE Transaction on Nanotechnology*, 12(4):498–507, May 2013.

[25] G. Csaba, P. Lugli, and W. Porod. Power Dissipation in Nanomagnetic Logic Devices. In *International Conference on Nanotechnology*, pages 346–348, Munic, Germany, 2004. IEEE.

[26] I. Ercan and N.G. Anderson. Heat dissipation bounds for nanocomputing: Theory and application to QCA. In *Nanotechnology (IEEE-NANO), 2011 11th IEEE Conference on*, pages 1289–1294, 2011.

[27] J. Das, S.M. Alam, and S. Bhanja. Ultra-Low Power Hybrid CMOS-Magnetic Logic Architecture . *Trans. on Computer And Systems*, 2011.

[28] B. Xu, R.G. Polcawich, S. Trolier-McKinstry, Y. Ye, and L.E. Cross. Sensing characteristics of in-plane polarized lead zirconate titanate thin films . *Applied Physics Letter*, 75(26), December 1999.

[29] T. Chung, S. Keller, and G.A. Carman. Electric-field-induced reversible magnetic single-domain evolution in a magnetoelectric thin film . *Applied Physics Letter*, (94), 2009.

[30] K. Roy, S. Bandyopadhyay, and J. Atulasimha. Switching dynamics of a magnetostrictive single- domain nanomagnet subjected to stress . *Phys. Rev. B*, (83):1–15, 2011.

[31] A. Aharoni. Demagnetizing factors for rectangular ferromagnetic prisms. *Journal of Applied Physics*, 83(6):3432–3434, March 1998.

[32] D.K. Karunaratne and S. Bhanja. Study of single layer and multilayer nano-magnetic logic architectures . *Journal Of Applied Physics*, (111), 2012.

[33] Comsol Multiphysics. http://www.comsol.com/.

[34] M. Vacca, M. Graziano, and M. Zamboni. Asynchronous Solutions for Nano-Magnetic Logic Circuits. *ACM J. on Emerging Tech. in Comp. Systems*, 7(4), December 2011.

[35] D.B. Carlton, N.C. Emley, E. Tuchfeld, and J. Bokor. Simulation Studies of Nanomagnet-Based Logic Architecture. *Nanoletters*, 8(12):4173–4178, November 2008.

[36] S. Guillon, D. Saya, L. Mazenq, L. Nicu, C. Soyer, J. Coste-calde, and D. Remiens. Lead-zirconate titanate (PZT) nanoscale patterning by ultraviolet-based lithography lift-off technique for nano-electromechanical systems applications . *2011 International Symposium on Piezoresponse Force Microscopy and Nanoscale Phenomena in Polar Materials*, July 2011.

[37] C. Huang, Y. Chen, Y. Liang, T. Wu, H. Chen, and W. Chao. Fabrication of Nanoscale PtOx /PZT/PtOx Capacitors by E-beam Lithography and Plasma Etching with Photoresist Mask . *Electrochemical and Solid-State Letters*, 2006.

[38] W. Scholz, J. Fidler, T. Schrefl, D. Suess, R. Dittrich, H. Forster, and V. Tsiantos. Scalable Parallel Micromagnetic Solvers for Magnetic Nanostructures. *Comp. Mat. Sci.*, (28):366–383, 2003.

Marco Vacca received the Dr.Eng. degree in electronics engineering from the Politecnico di Torino, Turin, Italy, in 2008. In 2013, he got the Ph.D. degree in electronics and communication engineering. He is currently working as an Research Assistant in the Politecnico di Torino. Since 2010, he has been teaching Design of Digital Circuits and Power Electronics. His research interests include quantum-dot cellular automata and others beyond-CMOS technologies.

Mariagrazia Graziano received the Dr.Eng. degree and the Ph.D in Electronics Engineering from the Politecnico di Torino, Italy, in 1997 and 2001, respectively. Since 2002 she is a researcher and since 2005 Assistant Professor at the Politecnico di Torino. Since 2008 she is adjunct Faculty at the University of Illinois at Chicago. Her research interests include design of CMOS "beyond CMOS" devices, circuits and architectures. She is author and co-author of more than 90 published works.

Luca Di Crescenzo received the Dr.Eng. degree in Electronics from the University of LAquila in 2010, magna cum laude. In 2012 he received the MoS degree in Electronics Engineering at the Polytechnic University of Turin. His main research interests include Physical Design Automation, custom architectures design for Machine Vision and Image Processing applications. He is currently working at T3LAB as a research engineer.

Alessandro Chiolerio received his Dr.Eng. degree in Materials Engineering in 2005 and his Ph.D. degree in Electron Devices in 2009 at Politecnico di Torino, Italy. Now he is Researcher at the Istituto Italiano di Tecnologia, doing research in the field of Smart Materials platform and functional nanocomposites for space sensor applications and flexible electronics. He is leader of 2 European, 1 regional and 1 industrial projects, co-author of more than 50 papers on international journals, 12 chapters and 5 patents.

Andrea Lamberti graduated in Physical Engineering at the Politecnico of Torino in 2009. In 2013 he received the PhD degree in Electronic Devices in the same institution working on metal-oxide nanostructures for energy applications. Currently, he is working as fellow researcher on the study of innovative materials and technological processes for the fabrication of M/NEMS biosensors.

Davide Balma received his Dr.Eng. in Physics of Advanced Technologies from University of Turin, Italy, in 2008 and his Ph.D. degree in Electronic Devices from Polytechnic of Turin in 2011. From January 2012 he is a post doc scientist at the EPFL and his research interests include MEMS fabrication technologies and piezoelectric materials and devices.

Giancarlo Canavese received his Dr.Eng. degree in Mechanical Engineering in 2004 and his Ph.D. degree in Biomedical Engineering in 2008 from Politecnico di Torino, Italy. He is a researcher at the Italian Institute of Technology in Torino. His areas of interest include piezoresistive composite materials, characterization of piezoelectric materials and devices, MEMS technologies and distribute tactile sensors for robotic applications.

Federica Celegato received her Dr.Eng. degree in Materials Science in 2003. From 2005 she works as Technical Collaborator to research activity at INRIM Electromagnetics Division, for characterization of magnetic thin films for spintronics. She has taken part in many international and national projects. She is co-author of about 60 publications.

Emanuele Enrico received the Dr. degree in physics from the Univerit di Torino, Turin, Italy, in 2008. In 2012 he got the Ph.D. degree in Metrology: Science and Techniques of the Measurements. He is currently working as a Technician in the Istituto Nazionale di Ricerca Metrologica and is vice-responsible of the laboratory Nanofacilty Piemonte. His research interests include quantum electronics and micro and nano fabrication technologies.

Paola Tiberto is a senior researcher at the Istituto Nazionale per la Ricerca Metrologica (INRIM) since 1994. She focused her scientific activity on phase transformation in metastable ferromagnetic alloys, magnetotransport properties of thin films and multilayer, study of magnetisation process in materials obtained by means of non-equilibrium technique, nanolithography process for patterning magnetic thin films. She is author of more than 170 scientific papers.

Luca Boarino received the Dr.Eng. in Physics in 1987 at University of Torino. He joined INRiM, working on photharmal spectroscopy in semiconductors, porous silicon and on gas doping in silicon nanostructures. From 2009 he is founder and responsible of Nanofacility Piemonte INRiM. He is author of more than 120 publications.

Maurizio Zamboni got his Dr.Eng. degree in 1983 and the Ph. D. degree in 1988 at the Politecnico di Torino. He joined the Electronics Department of the Politecnico di Torino in 1983 and he is now Full Professor of Electronics. His research activity focuses on multiprocessor architectures design, in IC optimization for Artificial Intelligence, low-power circuits and innovative beyond CMOS technologies. He is co-author of more than 120 scientific papers and three books.